Drug Design, Development and Therapy

Dovepress
open access to scientific and medical research

Open Access Full Text Article

ORIGINAL RESEARCH

Plumbagin promotes human hepatoma SMMC-7721 cell apoptosis via caspase-3/vimentin signal-mediated EMT

This article was published in the following Dove Press journal:
Drug Design, Development and Therapy

Yanfei Wei[1,*]
Beibei Lv[1,*]
Jinling Xie[2,*]
Yuan Zhang[3]
Yuning Lin[1]
Shengshan Wang[1]
Jing Zhong[1]
Yongxin Chen[1]
Yue Peng[1]
Jing Ma[1]

[1]Department of Physiology, Guangxi University of Chinese Medicine, Nanning, Guangxi 530200, People's Republic of China; [2]Medical Science Experimental Center, Guangxi University of Traditional Chinese Medicine, Nanning, Guangxi 530200, People's Republic of China; [3]Department of State Key Laboratory of Medicinal Chemical Biology and College of Pharmacy, Nankai University, Tianjin 710032, People's Republic of China

*These authors contributed equally to this work

Background/aims: Plumbagin (PL) has been shown to effectively inhibit tumor growth and migration of hepatocellular carcinoma cells in previous studies, but the specific mechanism for this remains unclear. The purpose of this study was to investigate the effects of PL-induced apoptosis in epithelial–mesenchymal transition (EMT) of human hepatocellular carcinoma (HCC) in vivo and in vitro.

Methods: SMMC-7721 cells were cultured, an EMT model was induced in vitro by TGF-β1, cell proliferation was detected by the MTT assay, cell invasion was analyzed by the Transwell invasion assay, and the apoptosis rate was measured by flow cytometry. RT-PCR was used to detect vimentin, E-cadherin, N-cadherin and snail mRNA, and Western blotting was used to detect the vimentin, caspase-3, PARP-1, E-cadherin, N-cadherin and snail protein expression levels. HE staining and TUNEL staining, immunohistochemistry and immunofluorescence were used to detect the expression levels of bax and bcl-2 in hepatocarcinoma xenografts and to evaluate their apoptosis in vivo.

Results: The in vitro results showed that PL inhibited the proliferation of EMT model cells, increased the apoptosis rate of the EMT model, and significantly decreased the vimentin, PARP-1, N-cadherin and snail protein levels, but significantly increased E-cadherin and caspase-3 protein expression. In addition, the in vivo results indicated that PL can affect the expression of bax/bcl-2 apoptotic marker proteins.

Conclusion: PL may induce apoptosis of human hepatocellular carcinoma cells undergoing epithelial–mesenchymal transition by increasing the caspase-3 protein level and cleaving vimentin.

Keywords: plumbagin, hepatocellular carcinoma, epithelial-mesenchymal transition, apoptosis, caspase-3

Introduction

Hepatocellular carcinoma (HCC) is one of the most commonly occurring cancers and is the second leading cause of cancer-related deaths from malignancy worldwide.[1] Despite advances in surgery and chemotherapy, HCC is associated with a poor 5-year survival rate due to its uncontrolled invasion and metastasis under the presently available treatments, including surgery and chemotherapy. Recurrence and metastasis are the major obstacles to improve survival for HCC patients.[2] Thus, there is a critical need for improving HCC therapies, which can be developed from the identification of new and effective chemotherapeutic agents and a better understanding of the molecular mechanisms involved.

Correspondence: Jing Ma
Department of Physiology, Guangxi University of Chinese Medicine, 13 Wuhe Road, Nanning, Guangxi 530001, People's Republic of China
Tel +86 771 473 3794
Email wenxin0815_2005@163.com

submit your manuscript | www.dovepress.com
DovePress
http://doi.org/10.2147/DDDT.S204787

Emerging evidence suggests that the epithelial-to-mesenchymal transition (EMT) is activated during HCC development, growth, progression, and metastasis.[3] It has been proposed that EMT facilitates metastatic dissemination of HCC cells from a primary organ to secondary sites; thus, intervention of this process may represent a novel strategy to prevent HCC metastasis. The expression of vimentin, along with the expression of mesenchymal markers, such as N-cadherin and the loss of E-cadherin, are key molecular markers of EMT.[4] A recent study found that vimentin, a core molecule in the EMT, is overexpressed in many epithelial-originating malignant tumor tissues or cancer cell lines (such as liver cancer and lung cancer). As an important signaling molecule, vimentin is involved in tumor cell growth, invasion and metastasis,[5,6] and when vimentin is cleaved by caspase, the cleaved fragments can be involved in tumor cellular apoptosis.[7] Hence, agents that can downregulate the activation of vimentin would have the potential to inhibit the development of cancer. Cells undergoing EMT become migratory, invasive and gain resistance to apoptosis. The failure of tumor cells to undergo apoptosis translates into malignancy potential and chemotherapeutic resistance.

A large number of phytochemicals are considered to regulate several molecular and metabolic processes, such as cell cycle regulation, apoptosis activation, angiogenesis and metastatic suppression, that can hinder cancer progression.[8,9] Plumbagin (5-hydroxy-2-methyl-1,4-napthoquinone, PL), an active naphthoquinone isolated from the roots of the medicinal plant *Plumbago zeylanica* L. (Figure 1A), is the main active ingredient of Plumbago.[10] PL has been demonstrated to have a wide spectrum of pharmacological effects, including anti-inflammatory, anti-angiogenesis, and anticancer, antibacterial, antifungal, hepatoprotective and neuroprotective effects in preclinical models. In recent years, the anticancer effect of PL has drawn a great deal of interest. PL has been shown to exert antitumor properties by inhibiting proliferation and inducing apoptosis in vitro in a broad range of cancer types, including breast cancer, non-small cell lung cancer, and HCC.[11–14] It also exhibits pro-apoptotic and radio-sensitizing activities in different tumor cells and animal models, both in vitro and in vivo. Currently, the anti-hepatoma effect of PL also causes widespread concern. In a previous study, PL was found to be cytotoxic against the HEPA-3B hepatoma cell line; the effect of PL on liver cancer inhibited the migration and invasion of the liver cancer cells through downregulation of MMP-2 and uPA. In addition, PL was found to induce significant regression of the tumors in a 3-methyl-4-dimethyl aminoazobenzene (3MeDAB)-induced hepatoma model in male Wistar rats. However, no studies exist regarding the effects of PL on apoptosis of epithelial–mesenchymal transition cells in HCC.

In this study, a human HCC xenograft model was established in nude mice, and an EMT model of liver cancer was generated from TGF-β stimulation. The effect of PL on the apoptosis of human HCC epithelial-mesenchymal transition cells was investigated to explore its potential mechanism of

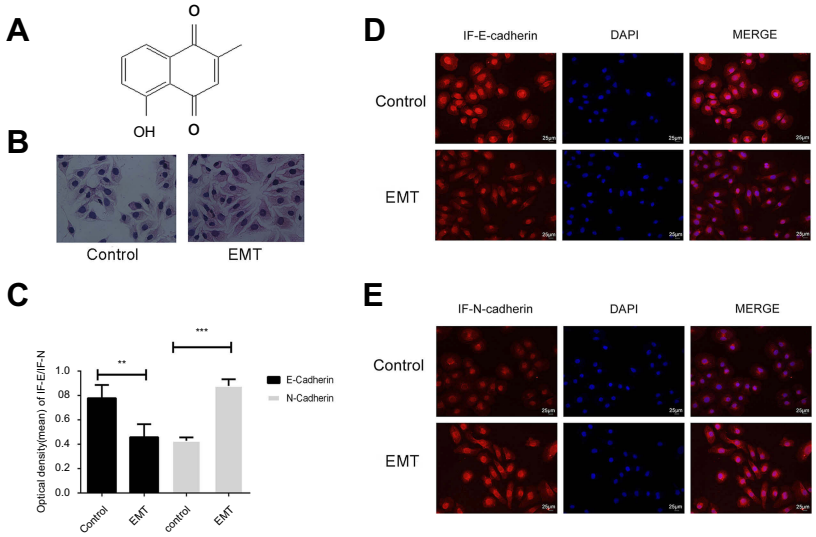

Figure 1 Chemical structure of plumbagin (PL) (**A**). SMMC-7221 cells were treated with10 ng/ml TGF-β1 for 48 h, EMT model preparation (**B**). The expression levels of E-cadherin and N-cadherin were detected by immunofluorescence to verify whether the EMT model was successfully established, error bars and mean ± SD, $^{**}P<0.01$, $^{***}P<0.001$ vs control group (**C**). The morphology of TGF-β-induced cells changed from a rounded shape to a fusiform shape. Cell nuclei were defined by DAPI (blue). Scale bar, 25 μm (**D, E**).

action to support the development of PL as a new candidate for effective HCC chemotherapy.

Materials and methods

Cell lines and animals

Plumbagin (PL) was purchased from Sigma-Aldrich Co. LLC (USA). Human hepatoma SMMC-7721 cells (Central South University of Advanced Research Center, Changsha, China) were cultured in Dulbecco's modified Eagle's medium (DMEM, Wisent) supplemented with 10% fetal bovine serum (FBS, Wisent), 100 U/ml penicillin and 100 μg/ml streptomycin in a hypoxic chamber (Sanyo, MCO-18AIC, Japan) adjusted to 5% CO_2 at 37 °C. Female BALB/C nu/nu mice (4-6-weeks-old; Hunan SJA Laboratory Animal Co., Ltd., Changsha, China) were housed in specific pathogen-free conditions. Since SMMC-7721 was not purchased from an approved commercial source, we confirmed that the use of this cell line was approved by the Ethics Committee of Guangxi University of Traditional Chinese Medicine.

Mice

SMMC-7721 cells were grown to approximately 80% confluency, and concentrated cells were regulated at a density of 2.5×10^7 cell/ml (the number of living cells in Trypan blue exclusion assay was over 95%). Nude mice were subcutaneously injected with 0.2 ml of cell suspension containing SMMC-7721; after approximately one week, round, small colliculi were observed (tumors of 0.5 cm^2 in diameter). The mice were randomly divided into 5 groups, which included the control group, positive thalidomide control group, and PL (Sigma, SLBG3436V, US) low-, middle-, and high-dose groups; each group had 6 nude mice. After tumor formation, the mice were peritoneally injected with normal saline (0.5 ml/d), thalidomide (200 mg/kg/d), or various concentrations of PL (1.25 mg/kg/d, 2.5 mg/kg/d, or 5 mg/kg/d). Each group was injected every other day. After 30 days, the tumor-bearing mice were sacrificed. The tumors were removed and fixed in 10% formaldehyde for pathological analysis and cell apoptosis. Procedures involving animals and their care were conducted in conformance with NIH guidelines (NIH Pub. No. 85-23, revised 1996) and were approved by the Animal Care and Use Committee of the Guangxi University of Chinese Medicine.

Cell culture and SMMC-7721 EMT model

Human hepatoma cells (SMMC-7721) were maintained in DMEM medium (HyClone, Utah, USA) containing 10% FBS. For experiments under hypoxic conditions, the cells were cultured in a hypoxic chamber adjusted to 5% CO_2 at 37 °C. The SMMC-7721 EMT model was established with 10 ng/ml TGF-β1 intervention at 48 h. Logarithmic growth phase SMMC-7721 and SMMC-7721 EMT model cells were used in the experiments.

Groups and treatment

EMT model cells in the logarithmic growth phase were divided into six groups: the EMT model group, 2 μM PL (μmol. L^{-1}) group, 4 μM PL group, 8 μM PL group, Vim cleavage group, and Caspease inhibitor group, wherein the culture was added to the EMT model group and cultured for 24 h. The PL groups were exposed to various concentrations of PL (2, 4 or 8 μM) for 24 h. The culture with 10 μmol/L withaferin-A (WFA, Santa Cruz, CA, USA) was added to the Vim cleavage group and cultured for 4 h. The culture with 10 $\mu mol\cdot L^{-1}$ Z-VAD-FMK (Selleck, TX, USA) was added to the Caspease inhibitor group and cultured for 24 h. The above experimental groups were compared with the control group for comparison of HCC. The liver cancer group was added to the culture and cultured for 24 h.

Cell proliferation assay

SMMC-7721 cells and EMT model cells were plated at a density of 4×10^3 cells/well in 96-well plates. After 24 h of culturing, the media was removed, and various drugs were added. The intervention was for 24 h and 48 h. MTT (5 mg/ml) (Sigma, St. Louis, MO) was added to the cells, and they were incubated for an additional 4 h at 37 °C. The supernatant was removed, and 100 μl of dimethyl sulfoxide (DMSO) (Sigma, St. Louis, Mo) was added to each well. The absorbance (OD value) was measured at a wavelength of 570 nanometers (nm).

Transwell assay

A BD Matrigel was diluted 4-fold in high-glucose DMEM, and 50 μl was added to each Transwell, followed by incubation for 3 h in the incubator. The SMMC-7721 cells and EMT model cells were cultured with serum-free high-glucose DMEM for 20 h, digested, and counted, adjusting the cell concentration to 2.5×10^4/100 μl. The cells were centrifuged and the supernatant was removed. The cells were resuspended with various drugs diluted in 100 μl of 0.1% BSA and were added to the Transwell chambers and placed in the incubator. The lower chamber contained 600 μl of 10% FBS culture medium, and the experiment was

performed in triplicate. After 24 h, the Transwell plate media was removed, and the cells were washed twice with PBS. The cells were fixed with 4% paraformaldehyde for 20 min, permeabilized with anhydrous formaldehyde for 20 min and stained with 0.1% crystal violet for 15 min. The cells were washed twice with PBS between each step. The Matrigel and cells that did not invade were gently removed with a cotton swab and mounted; five fields were randomly selected for observation and imaging under the inverted microscope, and the cell number was counted. The invasion inhibition rate = [1 - (number of invasive cells in the experimental group/the number of invasive cells in the control group)] ×100%.

Cellular apoptosis assay

Each group of cells was treated in strict accordance with the operating instructions of the apoptosis detection kit. The cells were digested with EDTA-free trypsin, centrifuged at 300 g a 4 °C for 5 min and collected. The cells were washed twice with precooled PBS, centrifuged at 300 g and 4 °C for 5 min, and 10–50×10^4 cells were collected. The cells were resuspended in 100 µl of 1×binding buffer, and then 5 µl of annexin V-FITC and 5 µl of PI staining solution were added, mixed gently, and incubated in the dark at room temperature for 10 min. Next, 400 µl of 1×binding buffer was added and mixed, and the sample was filtered with a nylon mesh (200 mesh) and added to a round-bottom flow cytometry tube. The cells were detected by flow cytometry within 1 h. The apoptosis rate = (number of apoptotic cells/total number of cells observed) ×100%.

RT-PCR

SMMC-7721 cells were harvested in medium containing 10% fetal bovine serum at a final concentration of 2×10^6 cells/mL and incubated for 24 hrs in 24-well plates. Next, plumbagin was added and the sample was incubated for 48 hrs. Total RNA was extracted from the SMMC-7721 cells by TRIzol reagent (Takara, Japan), and the total RNA content was measured by a Nano-100 differential spectrophotometer. The extracted 4.284 µg of RNA binds to reverse transcriptase to generate cDNA. The search for gene sequences and the primer design was conducted in-house, according to Gene Bank's guidelines. Real-time PCR for mRNA detection was performed using SYBR Green PCR Master Mix (Ambion, Carlsbad, CA, USA). The mRNA levels of E-cadherin, N-cadherin, vimentin and Snail were evaluated. The primer sets used for PCR amplification are as follows in Table 1.

Western blotting

Each group of cells was collected in the logarithmic growth phase (5–10×10^6 cell/ml). The cells were washed twice with cold PBS, and then 500 µl of cold lysate was added. After mixing, the cell sample was shaken at 4 °C for 15–20 min, and then centrifuged at 16,000 g and 4 °C for 15 min. The protein concentration of the supernatant was measured by the BCA method. Subsequently, 4×SDS sample treatment solution was added, and the samples were subjected to 100 °C heating for 5 min for denaturation. After SDS-PAGE electrophoresis, the proteins were transferred from SDS polyacrylamide gels to nitrocellulose (PVDF) membranes. After the transfer was completed, the PVDF membranes were blocked for1 h in 5% nonfat dry milk in TBST buffer at room temperature. The appropriate dilutions of primary antibodies were added as follows: mouse anti-caspase-3 (1:300, Santa Cruz, CA, USA, sc-7272), mouse anti-vimentin (1:300, Santa Cruz, CA, USA, sc-6260), mouse anti-PARP-1 (1:300, Santa Cruz, CA, USA,sc-8007), rabbit anti-β-actin

Table 1 mRNA gene primer sequences

Gene	Primer sequence		Product size/bp
Homo β-actin	Forward Reverse	5′-AGCGAGCATCCCCCAAAGTT-3′ 5′-GGGCACGAAGGCTCATCATT-3′	285 bp
Homo E-cadherin	Forward Reverse	5′-CGTAGCAGTGACGAATGTGG-3′ 5′-CTGGGCAGTGTAGGATGTGA-3′	175 bp
Homo N-cadherin	Forward Reverse	5'-CTTGCCAGAAAACTCCAGGG-3' 5'-TGTGCCCTCAAATGAAACCG-3'	213 bp
Homo vimentin	Forward Reverse	5'-TGAGTACCGGAGACAGGTGCAG-3' 5'-TAGCAGCTTCAACGGCAAAGTTC-3	119 bp
Homo Snail	Forward Reverse	5'-ATGCACATCCGAAGCCACA-3' 5'-TGACATCTGAGTGGGTCTGG-3'	190 bp

(1:1000, Cell Signaling Technology, USA, 13E5), rabbit anti-E-cadherin (1:1000, Cell Signaling Technology, USA, 3195), rabbit anti-N-cadherin (1:1000, Cell Signaling Technology, USA, 13116), rabbit anti-snail (1:1000, Cell Signaling Technology, USA, 3879) and then incubated overnight at 4 °C. The suitable secondary antibodies were then added, respectively: HRP-labeled goat anti-mouse IgG (1:12000) and goat anti-rabbit IgG (1:10000). The samples were then incubated at room temperature for 1 h. The CL chECL chemiluminescence method was utilized for visualization. X-ray film exposure, chemiluminescence development, film scanning, and quantitative analysis were conducted the US NIH ImageJ software. The anti-β-actin antibody was used as an internal loading control. The gray value ratio of the target band and internal loading control represent the results.

Histological assessment

The tumors were embedded in paraffin and stained with a Hematoxylin & Eosin Staining Kit to observe the morphological changes of liver cancer cells, the basement membrane integrity of the tumor angiogenesis, and the phenome apoptosis and necrosis in the tumor tissues. Cell apoptosis in tumor tissues was detected by the TUNEL assay using the conventional labeling index (LI), and 5 high-power fields were selected at 400X (Leica, DMI3000, Germany); all cells per high-power field were counted. The labeling index = the number of positive cells/horizons of all cells; the apoptosis index of each case (AI) equals the average horizon labeling index value.

Immunohistochemistry

To further detect the tumors tissue apoptosis levels, we next examined the apoptosis-related proteins Bax and Bcl-2 in hepatocellular carcinoma xenografts by immunohistochemistry. The tumor tissue sections were deparaffinized, rehydrated and boiled in 0.01 M sodium citrate for antigen retrieval. The endogenous peroxidase activity was quenched. The sections were incubated with rabbit anti-Bax (1:50, Sanying, Wuhan, China) and Bcl-2 (1:50, Abcam, Cambridge, MA) overnight at 4 °C. The sections were incubated with biotinylated secondary antibodies and a streptavidin-HRP complex (Zsbio, Wuhan, China). The staining was visualized using DAB (Boster, Wuhan, China). Representative images were taken using an Olympus camera (Nikon Instruments, Melvil). Optical density analysis was performed on the immunohistochemical images using IPP6.0 software. Four 400-fold images were taken for each slice to perform optical density analysis. The density was defined as the average optical density.

Immunofluorescence staining

Tissue from treated tumors was fixed with 4% paraformaldehyde for 25 min and permeabilized with 0.1% Triton X-100 for 10 min. The samples were then blocked with 2% bovine serum albumin (BSA) for 30 min at 37 °C, followed by incubation with primary antibody against Bax (1:50, Sanying, Wuhan, China) and Bcl-2 (1:50, Abcam, Cambridge, MA) at 4 °C overnight. The sections were subsequently incubated with the corresponding secondary antibody for 1 h at room temperature. The nuclei were stained with DAPI for 3 min, washed twice with PBS, and then images were captured using a DMI-4000B inverted fluorescence microscope (Olympus BX53). Fluorescence intensity analysis was performed on immunofluorescence images using IPP6.0 software. Three 400-fold images were selected for each slice for fluorescence intensity analysis, and the density (mean) was the average fluorescence intensity.

Statistical analysis

Statistical analysis was performed using SPSS 17.0. Comparisons between two groups were made using ANOVA, and each mean pairwise comparison was analyzed by using the q test. *P*-values are represented by * or #.

Results

Establishment and verification of the SMMC-7721 EMT model

To observe the morphological changes of the SMMC-7721 cells during EMT, HE staining was performed. The results showed that the control adherent cells grew well, and displayed an epithelioid form by fluorescence microscopy, and ovoid, polygonal or irregular shapes, such as stars. SMMC-7721 cells treated with 10 ng/ml TGF-β1 showed a slender morphology. The number of cells in the model group was significantly increased, and the cells exhibited a long spindle shape (Figure 1B). The expression levels of E-cadherin and N-cadherin were detected by immunofluorescence to verify whether the EMT model was successfully established. Epithelial–mesenchymal transition (EMT) mainly involved E-cadherin to N-cadherin translocation. The expression levels of E-cadherin and N-cadherin in SMMC-7721 cells treated with TGF-β1 for 48 hrs were then examined, as shown in Figure 1C–E. Compared with the control group, the E-cadherin expression levels were decreased and N-cadherin

expression levels were increased in SMMC-7721 cells treated with TGF-β1.

PL inhibits the proliferation of EMT induced by TGF-β in SMMC-7721 cells

To investigate the effects of PL in human HCC cells, SMMC-7721 cells were exposed to various concentrations of PL for 24 h and 48 h and then subjected to the 3-(4,5-dimethylthiazol-2-yl)-2,5-diphenyltetrazolium bromide (MTT) assay. PL was found to inhibit SMMC-7721 cell viability in a concentration- and time-dependent manner (Figure 2A). The inhibitory effect of the 24 h group was the most effective, so a 24 h intervention time was used in the follow-up experiments.

PL suppresses cell invasion of EMT induced by TGF-β in SMMC-7721 cells

Previous studies have shown the crucial role of PL in tumor cell proliferation, apoptosis, and migration.[15,16] The effect of PL on the invasion of SMMC-7721 cells induced by TGF-β in the EMT model was further determined in this study. In this study, cell invasion was measured by the Transwell invasion assay, and it was found that cell invasion was significantly reduced after PL treatment (Figure 2B and C). These results indicate that PL treatment inhibits cell invasion of SMMC-7721 cells after EMT.

PL induces apoptosis of EMT induced by TGF-β in SMMC-7721 cells

PL induced SMMC-7721 cell death, which was confirmed by annexin V/propidium iodide (PI) staining by flow cytometry. The annexin V/PI double-staining and flow cytometry results revealed that PL effectively induced the apoptosis of SMMC-7721 cells (Figure 3A and B). The proportion of apoptotic cells (lower right quadrant) significantly increased from 18.2% in untreated cells to 22.–50.6% in PL-treated

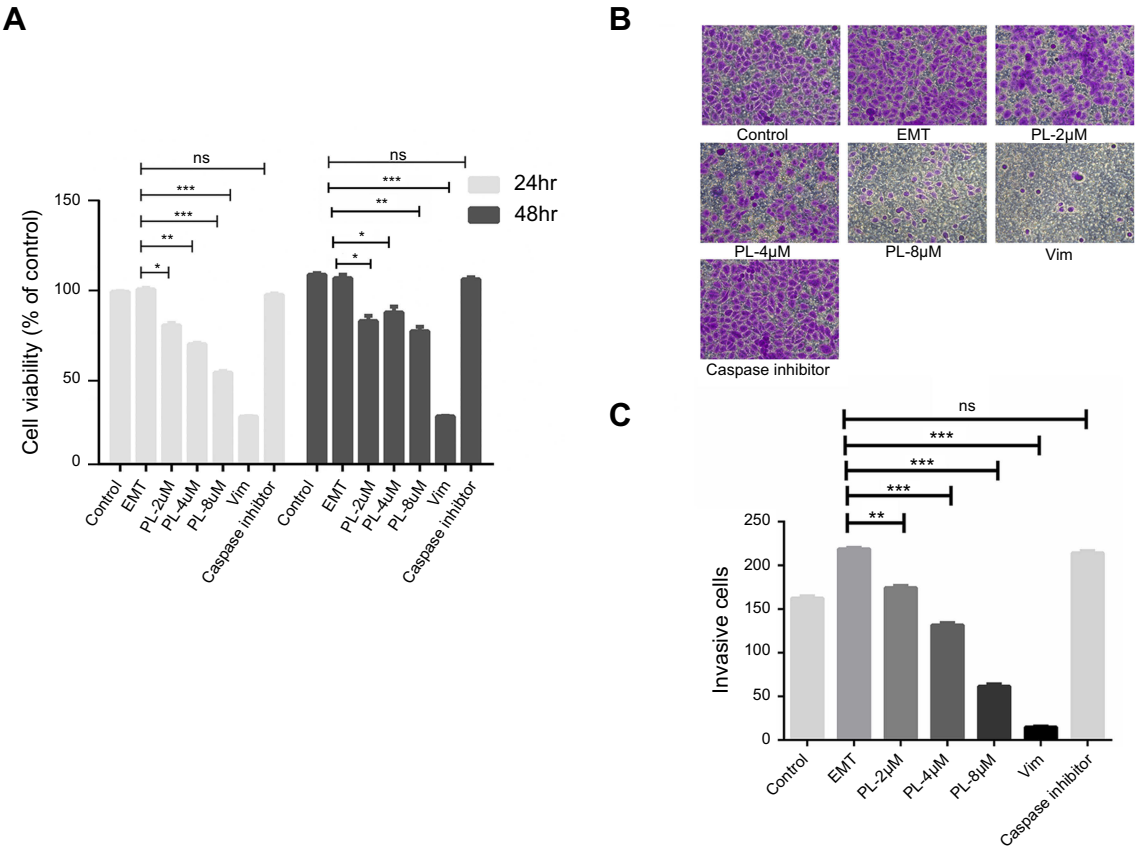

Figure 2 Cell viability of EMT cells treated with various concentrations of PL (2 μM, 4 μM, 8 μM), tumor angiogenesis inhibitor withaferin-A (WFA) (10 μmol·L-1), and caspase inhibitor (10 μmol·L-1) for 24 h or 48 h in a 5% CO_2 incubator at 37 °C. Cell viability is expressed as the percentage of control EMT. Each bar represents the mean value ± standard deviation (SD) of the intensity of fluorescent-positive cells during early apoptotic events of triplicate experiments. *P<0.05, **P<0.01, ***P<0.001, compared to the EMT cell group (**A**). The Transwell assay was performed to determine the invasive capacity of EMT cells (**B**). Cells treated with various concentrations of PL (2 μM, 4 μM, 8 μM), WFA (10 μmol·L-1) and caspase inhibitor (10 μmol·L-1) for 24 h in a 5% CO_2 incubator at 37 °C (**C**). Each bar represents the mean value ± standard deviation (SD) of the intensity of fluorescent-positive cells during early apoptotic events of triplicate experiments. *P<0.05, **P<0.01, ***P<0.001, compared to the EMT cell group.

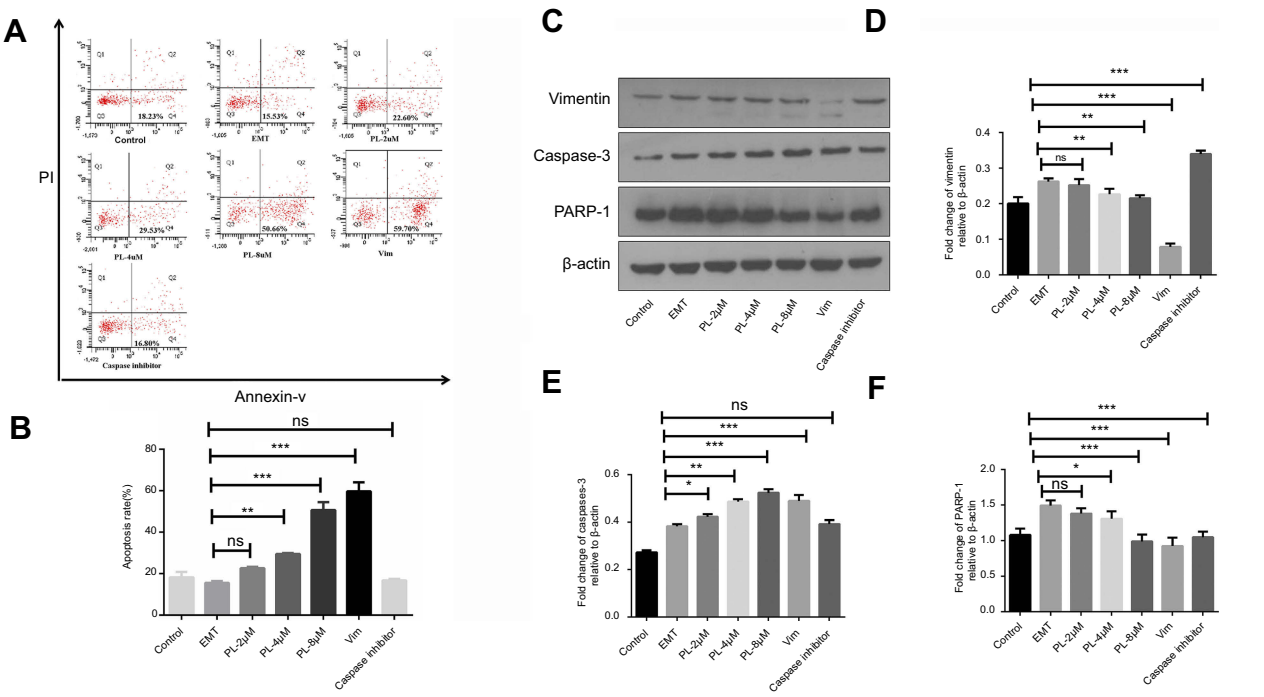

Figure 3 Effect of PL treatment on apoptosis in EMT cells (**A**). Cell apoptosis was detected using annexin V-FITC/propidium iodide (PI) staining and flow cytometry analysis. Fluorescence intensity of annexin V/FITC is plotted on the x-axis, and PI is plotted on the y-axis (**B**). The percentage of apoptotic cells examined by annexin V-FITC/PI staining and flow cytometry analysis. Each bar represents the mean value ± standard deviation (SD) of the intensity of fluorescent-positive cells during early apoptotic events of triplicate experiments. **P*<0.05, ***P*<0.01, ****P*<0.001, compared to the EMT cell group. Effect of PL, vim and caspase inhibitor treatment on vimentin, Caspase-3 and PARP-1 protein expression in MET cells (**C**). Protein expression of vimentin, caspase-3 and PARP-1 in EMT cells measured by Western blot analyses after treatment with PL, vim and caspase inhibitors. **β**-actin was used as a control housekeeping gene. The expression level of each protein is indicated (**D, E, F**). Densitometric analysis of vimentin, caspase-3 and PARP-1 relative to **β**-actin. Each bar represents the mean value ± standard deviation (SD) of the intensity of fluorescent-positive cells during early apoptotic events of triplicate experiments. **P*<0.05, ***P*<0.01, ****P*<0.001, compared to the EMT cell group.

cells. The proportion of necrotic cells did not significantly change after exposure to PL.

Regulation of PL on vimentin and apoptosis-related proteins

The mechanism of apoptosis induced by PL in epithelial-mesenchymal cells of human HCC was evaluated by measuring the level of apoptosis-related proteins. As shown in Figure 3C, compared with the EMT model group, PL treatment significantly decreased vimentin and PARP-1 protein expression and increased caspase-3 expression, especially in the 8 μM group, and the difference was significant (P<0.01). Some vimentin cleavage occurred in the 8 μM group and in the Vim group, and there was a positive correlation between the degree of cleavage and the rate of early apoptosis (Figure 3D–F).

Regulation of PL on vimentin and EMT-related proteins

The effect of PL on TGF-β-induced epithelial-mesenchymal transition in human HCC cells was assessed by measuring the expression levels of EMT-related genes and their proteins. As shown in Figure 4A–D, compared with the EMT model group, the expression of vimentin, N-cadherin and snail mRNA was significantly decreased after PL treatment, while the expression of E-cadherin was increased, especially in the 8 μM group, and the difference was significant (P<0.01). In addition, the results of Western blot analysis (Figure 4E–I) showed that the expression levels of vimentin, N-cadherin and snail proteins were significantly decreased after PL treatment compared with the EMT model group, while E-cadherin protein expression was increased, especially in the 8 μM high-dose group. These findings demonstrate that PL upregulates the expression of the epithelial biomarker E-cadherin, and downregulates the expression of the interstitial cell marker protein vimentin, N-cadherin and the transcriptional regulator Snail, thereby inhibiting the epithelial-mesenchymal transition of HCC in vitro.

Evaluation of apoptosis in vivo

To evaluate whether PL can induce apoptosis in vivo, tumor sections from mice were examined. In our previously

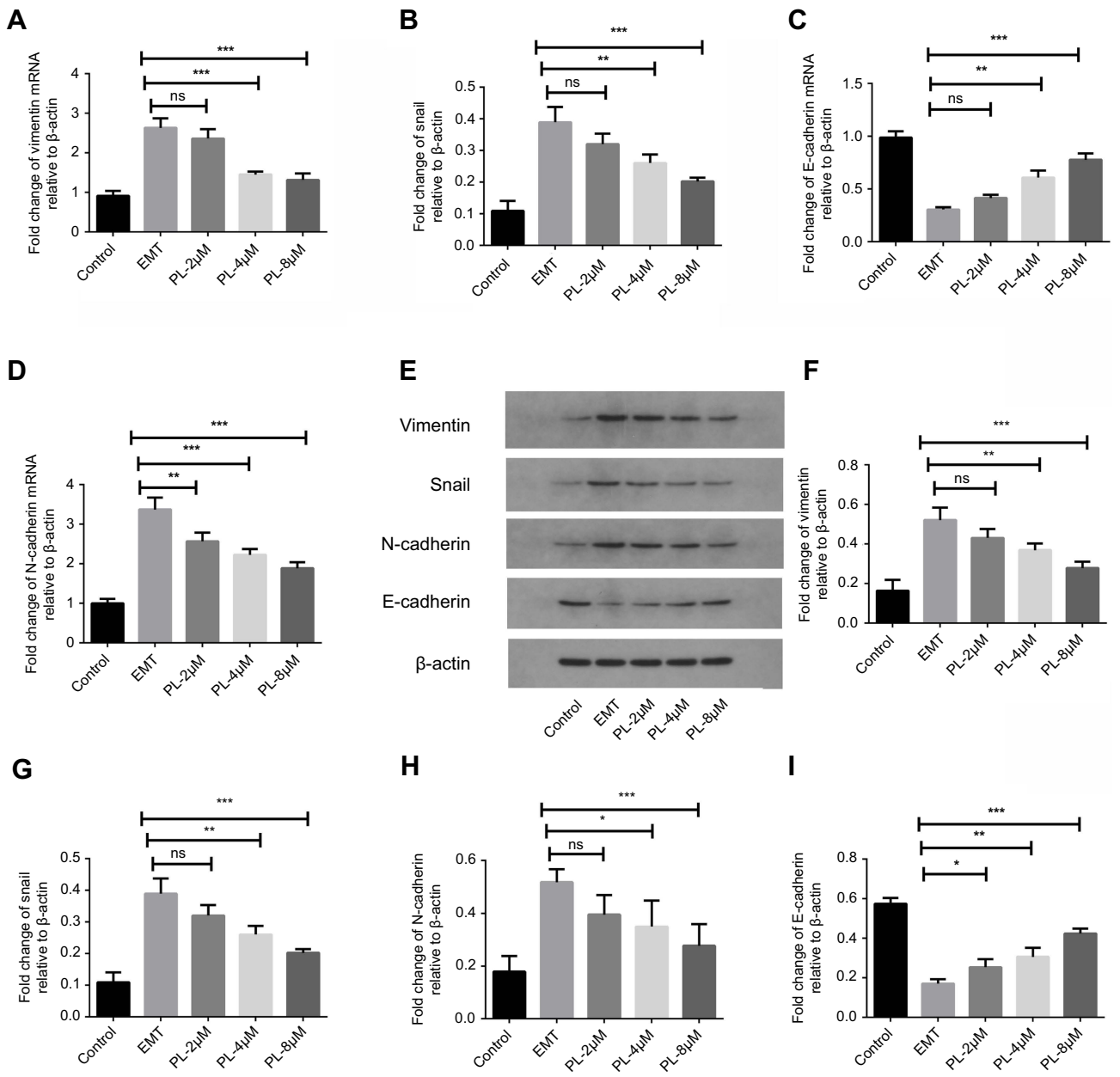

Figure 4 Effect of PL on the expression of vimentin, N-cadherin, E-cadherin and snail mRNA in SMMC-7721 cells induced by TGF-β as detected by RT-RCR. Bars and errors are relative to the EMT model group (**A-D**), mean ± SD, **P*<0.05, ***P*<0.01, ****P*<0.001. Protein expression levels of vimentin, N-cadherin, E-cadherin and snail in SMMC-7721 cells induced by TGF-β as measured by Western blot. Actin was used as an internal reference control. Represents the expression level (**E**) of each protein. Statistical analysis of vimentin, N-cadherin, E-cadherin and snail protein (**F-I**).Gray value analysis was performed relative to β-actin, N-cadherin, E-cadherin and snail. Each bar represents the mean ± standard deviation (SD) of TGF-β induction and different concentrations of PL-treated cells during triplicate experimental events. **P*<0.05, ***P*<0.01, ****P*<0.001, compared to the EMT model group.

published results, the growth curve of xenograft tumors showed that tumors treated with PL had significantly inhibited primary tumor growth compared with the control group, especially at the dose of 5 mg/kg/d ($P<0.05$). A slight time-dependent increase in relative tumor volume (RTV) was observed in the groups treated with either saline (0.5 ml/d) or PL (1.25, 2.5, and 5 mg/kg/d). The mean RTV values were 27.42, 21.64, 17.26, and 15.03. The relative tumor growth inhibition rate (TIR) obtained with PL was 6.40% at 1.25, 29.29% at 2.5, and 50.94% at 5 mg/kg/d.[12]

To determine whether PL induces apoptosis in human HCC cells. In the current study results, we measured apoptosis in tumor xenograft tissues using TUNEL staining. As shown in Figure 5A, the levels of apoptosis in the

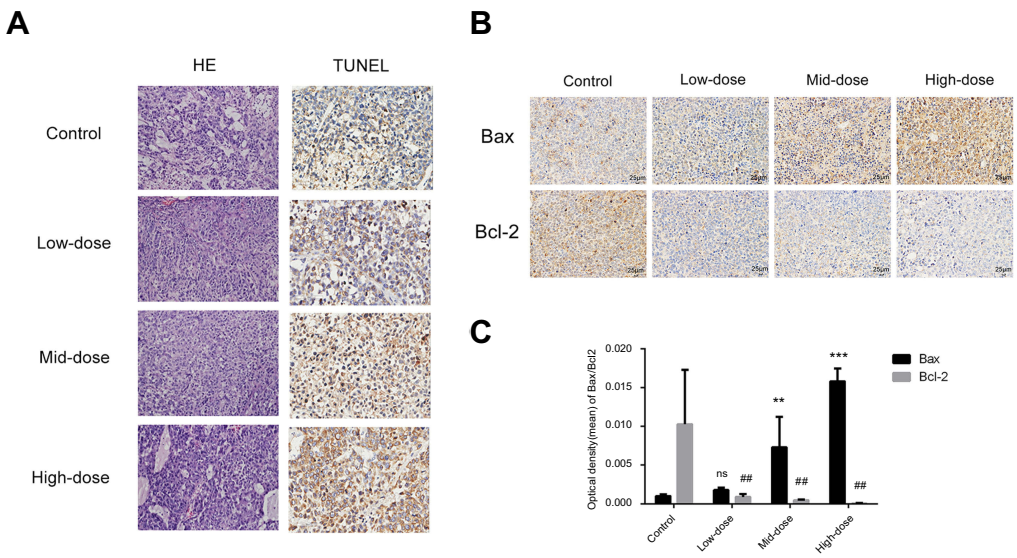

Figure 5 Histological analysis showing that PL inhibits tumor growth in vivo. The histological analysis of the livers of mice treated with PL for 30 days after treatment is shown (original magnification ×200). Tumor apoptosis was assessed by TUNEL using sections of tumors from mice treated with PL (1.25 mg/kg/d, 2.5 mg/kg/d, 5 mg/kg/d), saline (0.5 ml/d). The data represent the mean values of six mice ± SE (**A**). Immunohistochemical detection of Bax and Bcl-2 expression in hepatocellular carcinoma xenografts (**B**). Error bars and means ± SD, ***P*<0.01 vs Bax control group. #*P*<0.05, ##*P*<0.01 vs Bcl-2 control group, respectively (**C**).

PL treatment groups were greater than that in the model group. The results of HE showed that the cells in the model group had large nuclei, deep staining, obvious nuclear aberration, disordered arrangement without polarity, more striped arrangement, and obvious vascular hyperplasia; the cells in the model group were treated with a low dose of PL. Changes of the cells in the tumor as a whole were not obvious; however, the proliferation of blood vessels was obvious. When the PL dosage was raised, the proliferation of blood vessels decreased significantly and cell apoptosis became apparent, especially in the high-dose group. The expression of TUNEL was more obvious, where the positive expression of TUNEL was brownish. A light blue color was visible as nuclear staining. Compared with the model group, and there was no significant change in the low-dose PL group compared with the model group, indicating that the effect of the drug was positively correlated with the dose.

PL regulates apoptosis-related proteins in tumor tissues

Bcl-2 family proteins serve as importance regulators involved in apoptosis, acting to either inhibit or promote cell death. By analyzing the average optical density values of immunohistochemistry, as shown in Figure 5B and C, PL treatment significantly increased the expression of the pro-apoptotic protein Bax. It reduced the expression of the anti-apoptotic protein Bcl-2 in the membrane and cytoplasm of tumor cells compared to the control group. Among them, PL high dose group was the most significant ($P<0.001$). In addition, immunofluorescence assay showed that PL treatment reduced the nuclear immunofluorescence staining of Bcl-2 and increased the immunofluorescence staining of Bax (Figure 6A and B). By analyzing the average optical density of immunofluorescence, the expression of proapoptotic protein Bax was increased compared with the control group, and the PL high dose group was the most significant (P<0.001). In contrast, the expression of the anti-apoptotic protein Bcl-2 was significantly reduced (Figure 6C).

Discussion

The epithelial-mesenchymal transition (EMT) is a basic physiological and pathological phenomenon of organisms.[17] It refers to processes in which the epithelial cells acquire biological characteristics of mesenchymal cells, characterized by the loss of cell polarity, decreased expression of epithelial cell markers (such as E-cadherin) and increased expression of mesenchymal markers (eg, vimentin).[18] EMT plays a very important role in tumor invasion and metastasis and has become a hot topic of cancer research.[19,20]

As a marker of EMT, vimentin is an important cytoskeletal protein expressed in mesenchymal cells and some ectodermal cells. Vimentin, microtubules, actin and other proteins form a complete cellular support network system whose structure is characterized by radial distribution,

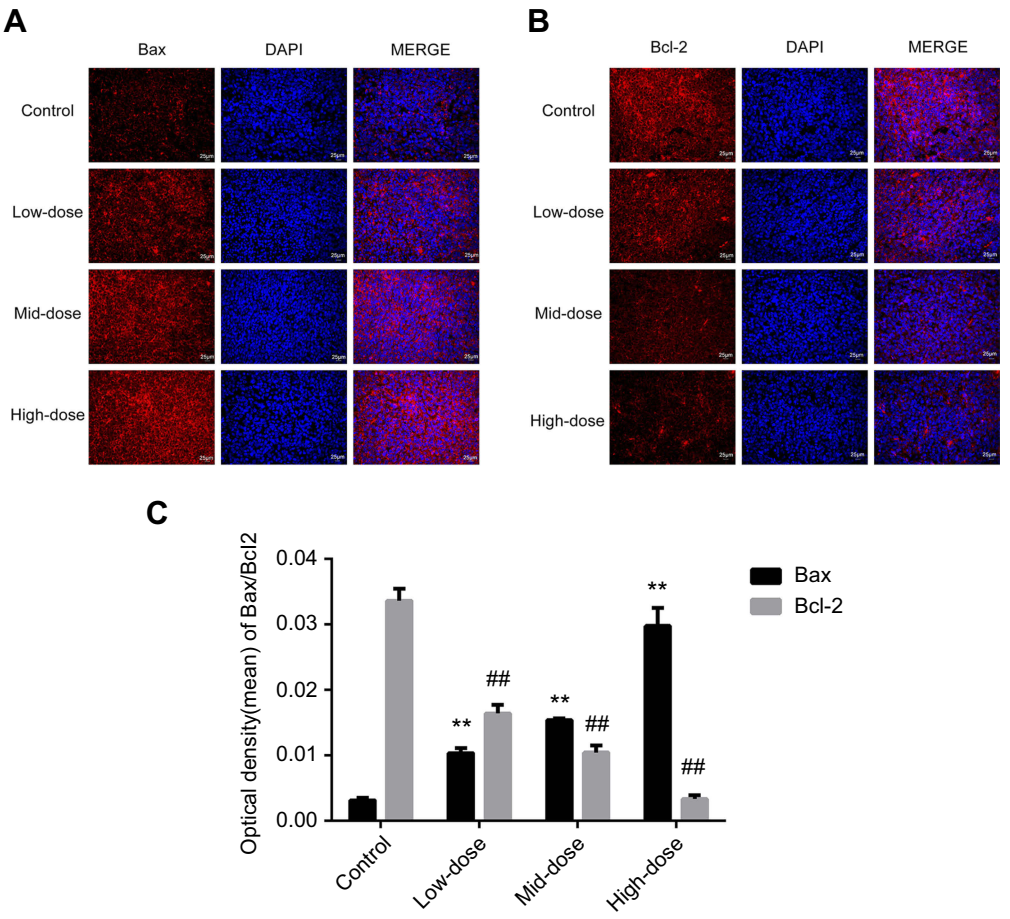

Figure 6 Immunofluorescence detection of Bax and Bcl-2 expression changes in TGF-β-induced hepatocellular carcinoma cells (400X). Cell nuclei were defined by DAPI (blue). Scale bar, 25 μm (**A, B**). Error bars and means ± SD, ***P*<0.01 vs Bax control group. #*P*<0.05, ##*P*<0.01 vs Bcl-2 control group (**C**).

connected to the nuclear membrane on the inside, and connected to the cell membrane on the outside, with microtubules, actin and many organelles in the middle. Therefore, vimentin has several intermediate fiber functions, such as cellular morphogenesis and maintenance, cellular displacement and spreading, nuclear localization and others.[21] In addition, the main function of vimentin also includes the effects of cell adhesion and migration and is also involved in signal transduction.[22] Recent studies have shown that vimentin is closely associated with the apoptosis caused by a variety of factors, especially those related to cancer research. Vimentin is cleaved into fragments of different sizes during apoptosis. Some studies[23] have found human leukemia cells (Jurkat cells) with anti-Fas antibody. After Fas stimulation, it was found that specific cleavage of vimentin can be used as an apoptosis marker for caspase activation. In the studies of human epithelial tumor cell apoptosis caused by ultraviolet radiation, some studies[24] have found that vimentin was cleaved into three fragments of different sizes. The cleavage of vimentin is an inevitable result of the process of apoptosis, and cleavage occurs in a cell type-specific manner.[25] Vimentin mediates apoptosis primarily by cleaving caspase. Cleavage of vimentin is an early apoptotic event, with poly ADP-ribose polymerase (poly ADP-ribose polymerase, PARP) cleavage occurring almost simultaneously. After vimentin undergoes structural damage, the N-terminal peptide produced from cleavage can further induce caspase-induced vimentin cleavage, promoting apoptosis signal amplification.[26] In the expression of the apoptosis pathway, PARP is produced by the activation of caspase-3. The results of the current study showed that among the hepatoma cells, the SMMC-7721 EMT model in the PL group and Vim cleavage group had increased caspase-3 protein levels, while vimentin and PARP-1 protein levels were reduced, showing a dose-dependency ($P<0.01$).

Regarding cancer therapeutics, many studies have been dedicated to developing anticancer drugs that target

vimentin. The tumor angiogenesis inhibitor, drunk eggplant hormone A (withaferin-A, WFA), targets vimentin, and WFA combined with vimentin causes covalent modification, inducing tumor cell apoptosis and thus exerting antitumor effects.[27] Silibinin and *Clerodendrum bungei* have strong anticancer activity and can inhibit prostate cancer invasion and metastasis by decreasing the expression of vimentin and reducing the activity of matrix metalloproteinase (MMP-2), thereby inhibiting prostate cancer invasion and metastasis.[28] The degree of vimentin reduction and proteolytic cleavage were consistent with the trend of the proliferation inhibition rate, invasion inhibition rate and early apoptosis rate of hepatoma cells. The proliferation inhibition rate, invasion inhibition rate and early apoptosis rate of cells in the Vim cleavage group were highest in the experimental group, while the proliferation inhibition rate, invasion inhibition rate and early apoptosis rate of cells in the Caspase inhibition group were lowest in the experimental group. Our experimental findings indicated that PL (especially the 8 μM group) could significantly reduce proliferation and invasion and induce hepatoma cell apoptosis. These effects of PL were related to vimentin reduction and caspase upregulation.

Tumor cell epithelial-mesenchymal transition is accompanied by changes in cell surface markers, including downregulation of the epithelial biomarker E-cadherin expression and upregulation of stromal cell marker proteins, such as vimentin and N-cadherin, and by transcriptional regulatory factors through Snail activation.[29] E-cadherin is a member of the calcium-dependent adhesion family. Decreased expression of E-cadherin leads to changes in cell morphology, decreased intercellular adhesion, and increased cellular activity, which occur during EMT, and is an important sign of, and plays an important role in, cancer infiltration.[30] Vimentin is an intermediate filament protein present in mesenchymal cells, which is positive in mesenchymal-derived tumor cells and negative in epithelial-derived tumor cells, so increased vimentin expression suggests tumor epithelial-mesenchymal transition. The expression of E-cadherin and Cytokeratin were seen to decrease. When the expression levels of N-cadherin and vimentin increased, the arrangement of the tumor cytoskeleton system changed, the biological characteristics of the cells changed, the adhesion function decreased, and it was becoming easier for the cells to detach from the primary tumor and invade or metastasize to surrounding tissues.[31] Snail is the first member of the Snail zinc finger protein family. Studies have shown that Snail is essentially a transcriptional repressor that directly inhibits E-cadherin expression by binding to the E-box junction motif of the E-cadherin promoter. In turn, EMT is induced to promote tumor invasion and distant metastasis.[32] The RT-PCR and Western blot results in this study showed that compared with the control group, the mRNA and protein expression levels of vimentin, N-cadherin and snail were induced and upregulated by TGF-β, while E-cadherin expression was downregulated. After PL treatment, compared with the EMT model group, the mRNA and protein expression levels of vimentin, N-cadherin and snail factors were downregulated, and the expression of E-cadherin was upregulated. The high dose of PL was the most effective. This indicates that PL can inhibit EMT. By inhibiting the expression levels of EMT-related proteins, PL can inhibit the occurrence and metastasis of HCC.

Anti-apoptosis genes (B-cell lymphoma-2, Bcl-2) and pro-apoptosis genes (Bax) have been shown to be important regulators of apoptosis in cancer cells.[33,34] The ratio between the pro-apoptotic protein bax and the anti-apoptotic protein Bcl-2 determines whether the cells survive or die.[35] In a preliminary experimental study, to evaluate the antitumor effect of PL in vivo, the SMMC-7221 tumor xenograft mouse model was used and found that PL inhibits the growth of SMMC-7221 cells in xenograft tumors in vivo and inhibits tumors. PL treatment inhibited tumor growth in a dose-dependent manner according to body weight. The Bcl-2 family proteins serve as importance regulators involved in apoptosis, acting to either inhibit or promote cell death. In this study, PL treatment significantly increased the pro-apoptosis Bax protein expression, whereas it decreased the anti-apoptosis Bcl-2 protein expression in both the membranes and cytoplasm of tumor cells compared to the control group. In addition, PL treatment reduced the nuclear immunofluorescence staining for Bcl-2, while increasing the nuclear immunofluorescence staining for Bax.

Thus, this study clearly indicated that PL increases caspase-3 protein levels and cleaves vimentin via the caspase/vimentin signaling pathway. PL induces the apoptosis of human HCC epithelial-mesenchymal transition cells, In our previous studies, we also found that PL has other mechanisms that inhibit HCC tumor angiogenesis, invasion and metastasis, and induce interaction between autophagy and apoptosis,[12,14] suggesting that PL is a potential anti-therapeutic drugs for

HCC, and provide more evidence for the clinical use of PL in the treatment of HCC.

Acknowledgments

The authors gratefully acknowledge financial support by the National Natural Science Foundation of China (No. 81760757, 81560690, 81403189), Guangxi Natural Science Foundation Major Project (No. 2017GXNSFAA198152), the Youth Innovation Team of Guangxi University of Traditional Chinese Medicine (2015QT001), the project of the Postgraduate Education Innovation Plan Topic of Guangxi (YCSY2018001), and the Guangxi Key Laboratory of Translational Medicine for Treating High-Incidence Infectious Diseases with Integrative Medicine.

Disclosure

The authors report no conflicts of interest in this work.

References

1. Bruix J, Gores GJ, Mazzaferro V. Hepatocellular carcinoma: clinical frontiers and perspectives. *Gut*. 2014;63(5):844–855. doi:10.1136/gutjnl-2013-306627
2. Yang A, Ju W, Yuan X, et al. Comparison between liver resection and liver transplantation on outcomes in patients with solitary hepatocellular carcinoma meeting UNOS criteria: a population-based study of the SEER database. *Oncotarget*. 2017;8(57):97428–97438. doi:10.18632/oncotarget.22134
3. Heerboth S, Housman G, Leary M, et al. EMT and tumor metastasis. *Clin Transl Med*. 2015;4:6. doi:10.1186/s40169-015-0048-3
4. Kölbl AC, Jeschke U, Andergassen U. The significance of epithelial-to-mesenchymal transition for circulating tumor cells. *Int J Mol Sci*. 2016;17(8):1308. doi:10.3390/ijms17081308
5. Lahat G, Zhu QS, Huang KL, et al. Vimentin is a novel anti-cancer therapeutic target; insights from in vitro and in vivo mice xenograft studies. *PLoS One*. 2010;5(4):e10105. doi:10.1371/journal.pone.0010105
6. Satelli A, Li S. Vimentin in cancer and its potential as a molecular target for cancer therapy. *Cell Mol Life Sci*. 2011;68(18):3033–3046. doi:10.1007/s00018-011-0735-1
7. Nakagawa H, Hikiba Y, Hirata Y, et al. Loss of liver E-cadherin induces sclerosing cholangitis and promotes carcinogenesis. *Proc Natl Acad Sci U S A*. 2014;111(3):1090–1095. doi:10.1073/pnas.1322731111
8. Iqbal J, Abbasi BA, Batool R, et al. Potential phytocompounds for developing breast cancer therapeutics: nature's healing touch. *Eur J Pharmacol*. 2018;827:125–148. doi:10.1016/j.ejphar.2018.03.007
9. Iqbal J, Abbasi BA, Mahmood T, et al. Plant-derived anticancer agents: a green anticancer approach. *Asian Pac J Trop Biomed*. 2017;7(12):1129–1150. doi:10.1016/j.apjtb.2017.10.016
10. Aziz MH, Dreckschmidt NE, Verma AK. Plumbagin, a medicinal plant-derived naphthoquinone, is a novel inhibitor of the growth and invasion of hormone-refractory prostate cancer. *Cancer Res*. 2008;68(21):9024–9032. doi:10.1158/0008-5472.CAN-08-2494
11. Li YC, He SM, He ZX, et al. Plumbagin induces apoptotic and autophagic cell death through inhibition of the PI3K/Akt/mTOR pathway in human non-small cell lung cancer cells. *Cancer Lett*. 2014;344(2):239–259. doi:10.1016/j.canlet.2013.11.001
12. Wei YF, Qi Y, Yuan Z, et al. Plumbagin restrains hepatocellular carcinoma angiogenesis by suppressing the migration and invasion of tumor-derived vascular endothelial cells. *Oncotarget*. 2017;8(9):15230.
13. Sagar S, Esau L, Moosa B, Khashab NM, Bajic VB, Kaur M. Cytotoxicity and apoptosis induced by a plumbagin derivative in estrogen positive MCF-7 breast cancer cells. *Anticancer Agents Med Chem*. 2014;14(1):170–180.
14. Lin Y, Chen Y, Wang S, et al. Plumbagin induces autophagy and apoptosis of SMMC-7721 cells in vitro and in vivo[J]. *J Cell Biochem*. 2019;120(6):9820–9830.
15. Checker R, Sharma D, Sandur SK, et al. Plumbagin inhibits proliferative and inflammatory responses of T cells independent of ROS generation but by modulating intracellular thiols. *J Cell Biochem*. 2010;110(5):1082–1093. doi:10.1002/jcb.22620
16. Subramaniya BR, Srinivasan G, Davis N, Subhadara LBR, Halagowder D, Sivasitambaram ND. Apoptosis inducing effect of plumbagin on colonic cancer cells depends on expression of COX-2. *PLoS One*. 2011;6(4):e18695. doi:10.1371/journal.pone.0018695
17. Yeung KT, Yang J. Epithelial-mesenchymal transition in tumor metastasis. *Mol Oncol*. 2017;11(1):28–39. doi:10.1002/1878-0261.12017
18. Chaw SY, Majeed AA, Dalley AJ, Chan A, Stein S, Farah CS. Epithelial to mesenchymal transition (EMT) biomarkers – E-cadherin, beta-catenin, APC and Vimentin – in oral squamous cell carcinogenesis and transformation. *Oral Oncol*. 2012;48(10):997–1006. doi:10.1016/j.oraloncology.2012.05.011
19. Lu J, Shenoy AK. Epithelial-to-pericyte transition in cancer. *Cancers*. 2017;9(7):77. doi:10.3390/cancers9070077
20. Shenoy AK, Jin Y, Luo H, et al. Epithelial-to-mesenchymal transition confers pericyte properties on cancer cells. *J Clin Investig*. 2016;126(11):4174–4186. doi:10.1172/JCI86623
21. Liu CY, Lin HH, Tang MJ, Wang YK. Vimentin contributes to epithelial-mesenchymal transition cancer cell mechanics by mediating cytoskeletal organization and focal adhesion maturation. *Oncotarget*. 2015;6(18):15966–15983. doi:10.18632/oncotarget.3862
22. Ivaska J, Pallari HM, Nevo J, Eriksson JE. Novel functions of vimentin in cell adhesion, migration, and signaling. *Exp Cell Res*. 2007;313(10):2050–2062. doi:10.1016/j.yexcr.2007.03.040
23. Morishima N. Changes in nuclear morphology during apoptosis correlate with vimentin cleavage by different caspases located either upstream or downstream of Bcl-2 action. *Genes Cells*. 2010;4(7):401–414. doi:10.1046/j.1365-2443.1999.00270.x
24. Hashimoto M, Inoue S, Ogawa S, et al. Rapid fragmentation of vimentin in human skin fibroblasts exposed to tamoxifen: a possible involvement of caspase-3. *Biochem Biophys Res Commun*. 1998;247(2):401. doi:10.1006/bbrc.1998.8799
25. Kwak HI, Kang H, Dave JM, et al. Calpain-mediated vimentin cleavage occurs upstream of MT1-MMP membrane translocation to facilitate endothelial sprout initiation. *Angiogenesis*. 2012;15(2):287–303. doi:10.1007/s10456-012-9262-4
26. Bonnomet A, Syne L, Brysse A, et al. A dynamic in vivo model of epithelial-to-mesenchymal transitions in circulating tumor cells and metastases of breast cancer. *Oncogene*. 2012;31(33):3741–3753. doi:10.1038/onc.2011.540
27. Bargagnamohan P, Hamza A, Kim YE, et al. The tumor inhibitor and antiangiogenic agent withaferin A targets the intermediate filament protein vimentin. *Chem Biol*. 2007;14(6):623–634. doi:10.1016/j.chembiol.2007.04.010
28. Fan JH. Silibinin inhibits prostate cancer invasion, motility and migration by suppressing vimentin and MMP-2 expression. *Chin Pharm Bull*. 2009;30(8):1162–1168.
29. Roy BC, Kohno T, Iwakawa R, et al. Involvement of LKB1 in epithelial–mesenchymal transition (EMT) of human lung cancer cells. *Lung Cancer*. 2010;70(2):136–145. doi:10.1016/j.lungcan.2010.02.004

30. Schmalhofer O, Brabletz S, E-cadherin T. beta-catenin, and ZEB1 in malignant progression of cancer. *Cancer Metast Rev*. 2009;28(1–2):151–166. doi:10.1007/s10555-008-9179-y
31. Balmer ML, Dufour JF. Biology of Hepatocellular Carcinoma In: Carr BI, editor. *Hepatocellular Carcinoma*. New York: Springer; 2011:21–34.
32. Franco-Chuaire ML, Magda Carolina SC, Chuaire-Noack L. Epithelial-mesenchymal transition (EMT): principles and clinical impact in cancer therapy. *Invest Clin*. 2013;54(2):186–205.
33. Yang J, Liu X, Bhalla K, et al. Prevention of apoptosis by Bcl-2: release of cytochrome c from mitochondria blocked. *Science*. 1997;275:1129–1132. doi:10.1126/science.275.5303.1129
34. Kim BM, Maeng K, Lee KH, Hong SH. Combined treatment with the Cox-2 inhibitor niflumic acid and PPARγ ligand ciglitazone induces ER stress/caspase-8-mediated apoptosis in human lung cancer cells. *Cancer Lett*. 2011;300(2):134–144. doi:10.1016/j.canlet.2010.09.014
35. Hanson CJ, Bootman MD, Distelhorst CW, Maraldi T, Roderick HL. The cellular concentration of Bcl-2 determines its pro- or anti-apoptotic effect. *Cell Calcium*. 2008;44(3):243–258. doi:10.1016/j.ceca.2007.11.014